

A model for pion collinear parton distribution function and form factor

Simone Venturini,^{1,2} Barbara Pasquini,^{1,2} and Simone Rodini³
(MAP Collaboration)*

¹*Dipartimento di Fisica, Università degli Studi di Pavia, I-27100 Pavia, Italy*

²*Istituto Nazionale di Fisica Nucleare, Sezione di Pavia, I-27100 Pavia, Italy*

³*CPHT, CNRS, Ecole Polytechnique, Institut Polytechnique de Paris, Route de Saclay, 91128 Palaiseau, France*
(Dated: July 21, 2023)

We developed a model for the pion light-front wave function (LFWF) that incorporates valence, sea and gluon degrees of freedom. Using the LFWF overlap representation, we derived parametrizations for the pion parton distribution functions and the electromagnetic form factor. These parametrizations depend on two distinct sets of parameters, enabling separate fits of the longitudinal- and transverse-momentum dependences of the LFWF. The pion PDFs are extracted from available Drell-Yan and photon-production data using the xFitter framework and are found well compatible with existing extractions. Furthermore, the fit of the electromagnetic form factor of the pion to all the available experimental data works quite successfully.

PRESENTED AT

DIS2023: XXX International Workshop on Deep-Inelastic Scattering and Related
Subjects,
Michigan State University, USA, 27-31 March 2023



I. LIGHT - FRONT WAVE FUNCTIONS OF THE PION

Light-front quantization is an effective approach in high-energy scattering, especially for describing the hadronic matrix elements that determine the soft contributions in inclusive and exclusive reactions. These matrix elements can be expressed through the overlap of light-front wave functions (LFWFs) associated with distinct parton configurations. Introducing the light-front Fock-state expansion and truncating the series up to the the four-partons components, the pion state can be represented as

$$|\pi(P)\rangle = |\pi(P)\rangle_{q\bar{q}} + |\pi(P)\rangle_{q\bar{q}g} + |\pi(P)\rangle_{q\bar{q}gg} + \sum_{\{\bar{s}\bar{s}\}} |\pi(P)\rangle_{q\bar{q}\{\bar{s}\bar{s}\}}, \quad (1)$$

where $q = u, d$ and the sum in $\{\bar{s}\bar{s}\}$ runs over the N_f -flavor pairs of the sea quarks ($u\bar{u}$, $d\bar{d}$, $s\bar{s}$ at the model scale). Restricting ourselves to consider only the contribution with zero orbital angular momentum, the LFWF for each Fock-state component in Eq. (1) can be written in a model independent way in terms of light-front wave-amplitudes (LFWAs) as [1]

$$|\pi(P)\rangle_{q\bar{q}}^{l_z=0} = \int d[1]d[2] \frac{\delta_{c_1 c_2}}{\sqrt{3}} \psi_{q\bar{q}}^{(1)}(1, 2) \left[q_{c_1\uparrow}^\dagger(1) \bar{q}_{c_2\downarrow}^\dagger(2) - q_{c_1\downarrow}^\dagger(1) \bar{q}_{c_2\uparrow}^\dagger(2) \right] |0\rangle, \quad (2)$$

* The MAP acronym stands for “Multi-dimensional Analyses of Partonic distributions”. It refers to a collaboration aimed at studying the three-dimensional structure of hadrons.

$$|\pi(P)\rangle_{q\bar{q}g}^{l_z=0} = \int d[1]d[2]d[3] \frac{T_{c_1 c_2}^a}{2} \psi_{q\bar{q}g}^{(1)}(1, 2, 3) \left[(q\bar{q})_{A,1}^\dagger g_{a\downarrow}^\dagger(3) - (q\bar{q})_{A,-1}^\dagger g_{a\uparrow}^\dagger(3) \right] |0\rangle, \quad (3)$$

$$\begin{aligned} |\pi(P)\rangle_{q\bar{q}gg}^{l_z=0} &= \int d[1]d[2]d[3]d[4] \frac{\delta_{c_1 c_2} \delta^{ab}}{\sqrt{24}} \left\{ \psi_{q\bar{q}gg}^{(1)}(1, 2, 3, 4) (q\bar{q})_{A,0}^\dagger (gg)_{S,0}^\dagger \right. \\ &\quad \left. + \psi_{q\bar{q}gg}^{(2)}(1, 2, 3, 4) (q\bar{q})_{S,0}^\dagger (gg)_{A,0}^\dagger \right\} |0\rangle, \end{aligned} \quad (4)$$

$$\begin{aligned} |\pi(P)\rangle_{q\bar{q}\{\delta\bar{\delta}\}}^{l_z=0} &= \int d[1]d[2]d[3]d[4] \frac{\delta_{c_1 c_2} \delta_{c_3 c_4}}{3} \left\{ \psi_{q\bar{q}\delta\bar{\delta}}^{(1)}(1, 2, 3, 4) (q\bar{q})_{A,0}^\dagger (\delta\bar{\delta})_{S,0}^\dagger \right. \\ &\quad \left. + \psi_{q\bar{q}\delta\bar{\delta}}^{(2)}(1, 2, 3, 4) (q\bar{q})_{S,0}^\dagger (\delta\bar{\delta})_{A,0}^\dagger \right. \\ &\quad \left. + \psi_{q\bar{q}\delta\bar{\delta}}^{(3)}(1, 2, 3, 4) \left[(q\bar{q})_{A,1}^\dagger (\delta\bar{\delta})_{A,-1}^\dagger - (q\bar{q})_{A,-1}^\dagger (\delta\bar{\delta})_{A,1}^\dagger \right] \right\} |0\rangle. \end{aligned} \quad (5)$$

The measures in Eqs. (2)-(5) are defined as:

$$\prod_{i=1}^N d[i] = [dx]_N [d^2\mathbf{k}_\perp]_N, \quad (6)$$

$$[dx]_N = \prod_{i=1}^N \frac{dx_i}{\sqrt{x_i}} \delta\left(1 - \sum_{i=1}^N x_i\right), \quad [d^2\mathbf{k}_\perp]_N = \frac{1}{[2(2\pi)^3]^{N-1}} \prod_{i=1}^N d^2\mathbf{k}_{\perp i} \delta^{(2)}\left(\sum_{i=1}^N \mathbf{k}_{\perp i}\right). \quad (7)$$

The LFWAs $\psi_\beta^{(i)}$ are generic functions depending on $i = (x_i, \mathbf{k}_{\perp i})$, where x_i and $\mathbf{k}_{\perp i}$ are, respectively, the fraction of pion momentum in the collinear direction carried by the i -th parton and the transverse momentum of the i -th parton. Furthermore, $q_{c\lambda}^\dagger$, $\bar{q}_{c\lambda}^\dagger$ and $g_{a\lambda}^\dagger$ are creation operator of quarks, antiquarks and gluons, respectively, and are labelled by the specific quantum numbers of the partons: the color (c and a), the helicity ($\lambda = \uparrow$ or \downarrow), and, in case of the fermions, the flavor q . For brevity, in Eqs. (2)-(5) we introduced the operators $(p_1 p_2)_{A/S,0/1}^\dagger$: these are anti-symmetric (A) or symmetric (S) combinations of creation operators of the partons p_1 and p_2 with total helicity 0 or 1. The subscript $\delta\bar{\delta}$ refers to the sea quarks $u\bar{u}$, $d\bar{d}$, $s\bar{s}$ and $T_{ij}^a = \frac{\lambda_{ij}^a}{2}$ represent the SU(3) color matrices. The quark and gluon PDFs of the pion are defined as

$$f_1^q(x) = \int \frac{dz^-}{2(2\pi)} e^{ik^+ z^-} \langle \pi(p) | \bar{\psi}(0) \gamma^+ \psi(z) | \pi(p) \rangle \Big|_{\substack{z^+=0 \\ \mathbf{z}_\perp=0}}, \quad (8)$$

$$f_1^g(x) = \frac{1}{xp^+} \int \frac{dz^-}{2\pi} e^{ik^+ z^-} \langle \pi(p) | G^{+\mu}(0) G_{\mu+}(z) | \pi(p) \rangle \Big|_{\substack{z^+=0 \\ \mathbf{z}_\perp=0}}, \quad (9)$$

where ψ is the quark field and $G^{\mu\nu}$ is the gluon field strength tensor. By inserting in Eqs. (8) and (9) the pion state of Eq. (1), one obtains the representation of the pion PDFs in terms of overlap of LFWFs for each Fock-state component, as given in Ref. [2]. Moreover, by neglecting electroweak corrections and quark masses, charge symmetry imposes $f_{1,\pi^+}^u = f_{1,\pi^+}^{\bar{d}} = f_{1,\pi^+}^d = f_{1,\pi^+}^{\bar{u}} = 2f_{1,\pi^0}^u = 2f_{1,\pi^0}^{\bar{u}} = 2f_{1,\pi^0}^d = 2f_{1,\pi^0}^{\bar{d}}$. Hereafter, we will refer to distributions in positively charged pions. Assuming also a SU(3)-symmetric sea, i.e., $f_1^u = f_1^{\bar{d}} = f_1^s = f_1^{\bar{s}}$, we will consider three independent PDFs: the total valence contribution f_1^v , the total sea contribution f_1^S , given by

$$\begin{aligned} f_1^v &= f_1^{u_v} - f_1^{d_v} = (f_1^u - f_1^{\bar{u}}) - (f_1^d - f_1^{\bar{d}}) = 2f_1^{u_v}, \\ f_1^S &= 2f_1^u + 2f_1^{\bar{d}} + f_1^s + f_1^{\bar{s}} = 6f_1^u, \end{aligned} \quad (10)$$

and the gluon contribution f_1^g .

As discussed in Ref. [2], we can analogously obtain the LFWF overlap representation for the pion e.m. form factor, starting from the definition

$$F_\pi(Q^2) = \frac{1}{(p+p')^+} \langle \pi(p') | \bar{\psi}(0) \gamma^+ \psi(0) | \pi(p) \rangle \quad (11)$$

where $Q^2 = -q^2 > 0$ and $q = p' - p$ is the four-momentum transfer.

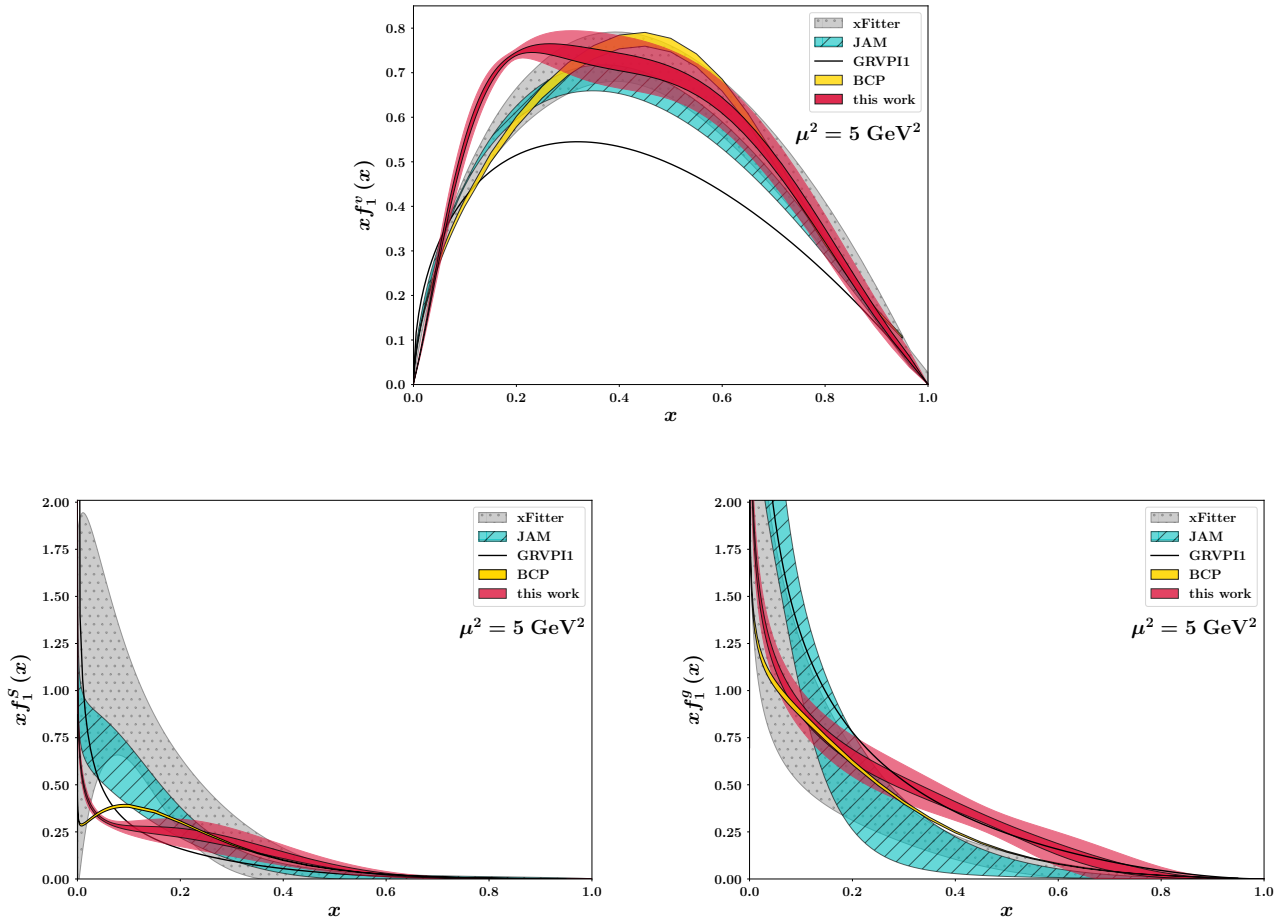


FIG. 1. $x f_1$ as function of x for the total valence (upper panel), total sea (left panel in the bottom) and gluon (right panel in the bottom) contributions at $\mu^2 = 5 \text{ GeV}^2$. The light (dark) red bands show the results of this work with the 3σ (1σ) uncertainty in comparison with the results from the JAM collaboration [3] (light blue bands), the analysis of xFitter collaboration [4] (grey bands), the BCP fit of Ref. [5] (yellow bands) and the GRVPI1 fit [6] (solid black curves).

A. Parametrization

We have designed the LFWAs in such a way that the parameters associated with longitudinal and transverse momentum dependence are treated separately during the fitting process of the pion PDFs and electromagnetic (e.m.) form factor (FF). Specifically, the LFWAs are written in the following general form

$$\psi_\beta^{(i)}(1, 2, \dots, N) = \phi_\beta^{(i)}(x_1, x_2, \dots, x_N) \Omega_\beta^{(i)}(x_1, \mathbf{k}_{\perp 1}, x_2, \mathbf{k}_{\perp 2}, \dots, x_N, \mathbf{k}_{\perp N}), \quad (12)$$

where the functions $\phi_\beta^{(i)}$ can be expressed as a linear combination of pion distribution amplitudes and $\Omega_\beta^{(i)}$ are modified x -dependent gaussian functions. The last ones are normalized in such a way that the fit of the collinear PDFs does not contain any spurious dependence of the parameters in the transverse-momentum space. In total the model has a set \mathcal{X} of six parameters for the longitudinal momentum dependence, fitted to pion PDFs, and a set \mathcal{A} of four parameters for the transverse momentum dependence, constrained from the fit to the pion e.m. FF.

II. EXTRACTION OF THE PION PDF AND ELECTROMAGNETIC FORM FACTOR

The fit of the pion PDFs has been performed by using the open-source tool xFitter [4, 7]. The data included in the analysis are from the NA10 [8], E615 [9] and WA70 [10] experiments. The complete data set has been cut to exclude

the kinematic region corresponding to the J/ψ and Υ resonances. We fixed the initial scale to $\mu_0 = 0.85$ GeV and the factorization scale μ_F and renormalization scale μ_R to $\mu_F = \mu_R = 0.8$ GeV. The reduced chi-squared from a single minimization is $\hat{\chi}^2/N_{d.o.f.} = 0.88$ for the number of degrees of freedom $N_{d.o.f.} = 260 - 6 = 254$. The fit to the real data has been repeated 1000 times varying the experimental points by random gaussian shifts both for the statistic and systematic uncertainties, thus obtaining 1000 bootstrap replicas. The renormalization scale and the factorization scale have been varied replica by replica in a way such that $\mu_0 \leq \mu_F \leq \mu_0$ and $\mu_0 \leq \mu_R \leq 2\mu_0$.

In Fig. 1 we show our results for the pion PDFs (red bands) at the scales of $\mu^2 = 5$ GeV² in comparison with different analyses: the GRVPI1 solution [6] (solid black curves); the xFitter results [4] (grey bands); the JAM extraction [3] (light blue bands); the results within the statistical model of Bourrely-Chang-Peng (BCP) (Bourrely [5] (yellow bands). Overall, the modern analyses give compatible results within the relative error bands. The agreement is better for the valence and sea contributions at larger x and for the gluon PDF in the small x region.

For the fit of the FF, we included 100 experimental points in a Q^2 range from 0.015 GeV² to 9.77 GeV², corresponding to the experimental measurements described in the legend of Fig. 2. The FF depends both on the set \mathcal{X} , fixed from the pion PDF fit, and the set \mathcal{A} , which contains four distinct elements to be determined from the FF fit. The bootstrap replica method is used to propagate both the experimental uncertainties and the uncertainties associated to the parameters of the set \mathcal{X} that are not directly free fitting variables. The method is described in detail in Ref. [2]. In the end, the best fit produces a reduced chi-squared of 1.19.

In Fig. 2, we show the results for the square of the pion e.m. form factor with the inner (dark blue) band representing the 68% uncertainty and the external (light blue) band showing the 99.7% uncertainty. Agreement with the different data sets is qualitatively evident. We stress that the two bands incorporate the error propagation of the PDF parameters, representing therefore more than just the experimental uncertainty on the FF.

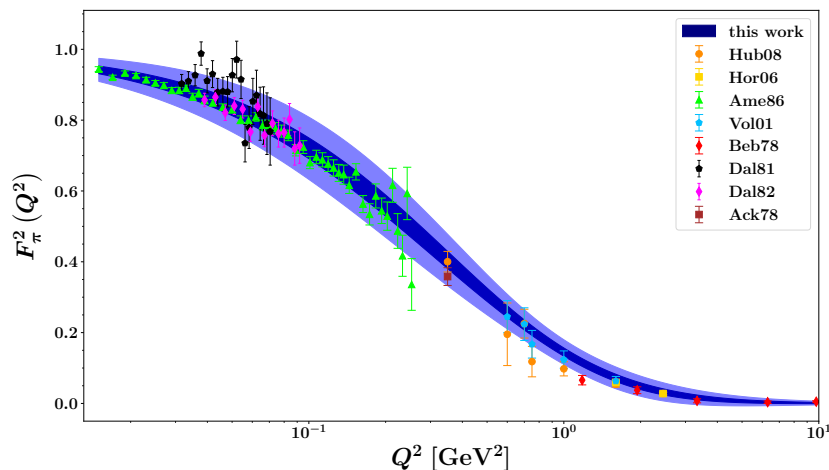


FIG. 2. Fit results for the square of the pion electromagnetic form factor as function of Q^2 . The dark (light) blue band shows the 68% (99.7%) of the replicas. The experimental data correspond to Hub08 [11], Hor06 [12], Ame86 [13], Vol01 [14], Beb78 [15], Dal82 [16, 17], Ack78 [18].

III. CONCLUSIONS

In this study, we have presented an extraction of the pion PDFs and e.m. FF using a light-front model approach that incorporates contributions from valence quarks, sea quarks, and gluons. We have developed a model for the pion LFWFs, ensuring that the fit of the collinear PDFs remains free from any spurious dependence on the parameters in the transverse-momentum space. These parameters are separately fitted to the available data on the pion e.m. form factor. The approach presented in this study serves as a proof-of-principle for achieving a unified description of hadron distribution functions, encompassing both the longitudinal and transverse momentum dynamics of partons within hadrons. The ultimate objective is to extend this framework to incorporate transverse-momentum dependent parton distributions (TMDs) and generalized parton distributions (GPDs) in a global fit. This will leverage the wealth of data expected from upcoming experiments at JLab, COMPASS++/AMBER, and future electron-ion colliders,

taking the analysis a step further than previous studies that have only considered simultaneous PDFs and TMDs analysis [19], or have focused solely on TMDs [20, 21], and GPDs [22] separately.

-
- [1] Xiang-dong Ji, Jian-Ping Ma, and Feng Yuan. Classification and asymptotic scaling of hadrons' light cone wave function amplitudes. *Eur. Phys. J. C*, 33:75–90, 2004. doi:10.1140/epjc/s2003-01563-y.
- [2] Barbara Pasquini, Simone Rodini, and Simone Venturini. Valence quark, sea, and gluon content of the pion from the parton distribution functions and the electromagnetic form factor. *Phys. Rev. D*, 107(11):114023, 2023. doi:10.1103/PhysRevD.107.114023.
- [3] P. C. Barry, Chueng-Ryong Ji, N. Sato, and W. Melnitchouk. Global QCD Analysis of Pion Parton Distributions with Threshold Resummation. *Phys. Rev. Lett.*, 127(23):232001, 2021. doi:10.1103/PhysRevLett.127.232001.
- [4] Ivan Novikov et al. Parton Distribution Functions of the Charged Pion Within The xFitter Framework. *Phys. Rev. D*, 102(1):014040, 2020. doi:10.1103/PhysRevD.102.014040.
- [5] Claude Bourrely, Wen-Chen Chang, and Jen-Chieh Peng. Pion Partonic Distributions in the Statistical Model from Pion-induced Drell-Yan and J/Ψ Production Data. *Phys. Rev. D*, 105(7):076018, 2022. doi:10.1103/PhysRevD.105.076018.
- [6] M. Gluck, E. Reya, and A. Vogt. Pionic parton distributions. *Z. Phys. C*, 53:651–656, 1992. doi:10.1007/BF01559743.
- [7] S. Alekhin et al. HERAFitter. *Eur. Phys. J. C*, 75(7):304, 2015. doi:10.1140/epjc/s10052-015-3480-z.
- [8] B. Betev et al. Differential Cross-section of High Mass Muon Pairs Produced by a 194-GeV/ $c\pi^-$ Beam on a Tungsten Target. *Z. Phys. C*, 28:9, 1985. doi:10.1007/BF01550243.
- [9] J. S. Conway et al. Experimental Study of Muon Pairs Produced by 252-GeV Pions on Tungsten. *Phys. Rev. D*, 39:92–122, 1989. doi:10.1103/PhysRevD.39.92.
- [10] M. Bonesini et al. High Transverse Momentum Prompt Photon Production by π^- and π^+ on Protons at 280-GeV/c. *Z. Phys. C*, 37:535, 1988. doi:10.1007/BF01549712.
- [11] G. M. Huber et al. Charged pion form-factor between $Q^2 = 0.60 \text{ GeV}^2$ and 2.45 GeV^2 . II. Determination of, and results for, the pion form-factor. *Phys. Rev. C*, 78:045203, 2008. doi:10.1103/PhysRevC.78.045203.
- [12] T. Horn et al. Determination of the Charged Pion Form Factor at $Q^2 = 1.60$ and 2.45-(GeV/c)^2 . *Phys. Rev. Lett.*, 97:192001, 2006. doi:10.1103/PhysRevLett.97.192001.
- [13] S. R. Amendolia et al. A Measurement of the Space - Like Pion Electromagnetic Form-Factor. *Nucl. Phys. B*, 277:168, 1986. doi:10.1016/0550-3213(86)90437-2.
- [14] J. Volmer et al. Measurement of the Charged Pion Electromagnetic Form-Factor. *Phys. Rev. Lett.*, 86:1713–1716, 2001. doi:10.1103/PhysRevLett.86.1713.
- [15] C. J. Bebek et al. Electroproduction of single pions at low epsilon and a measurement of the pion form-factor up to $q^2 = 10 \text{ GeV}^2$. *Phys. Rev. D*, 17:1693, 1978. doi:10.1103/PhysRevD.17.1693.
- [16] E. B. Dally et al. Measurement of the π^- Form-factor. *Phys. Rev. D*, 24:1718–1735, 1981. doi:10.1103/PhysRevD.24.1718.
- [17] E. B. Dally et al. Elastic Scattering Measurement of the Negative Pion Radius. *Phys. Rev. Lett.*, 48:375–378, 1982. doi:10.1103/PhysRevLett.48.375.
- [18] H. Ackermann, T. Azemoon, W. Gabriel, H. D. Mertiens, H. D. Reich, G. Specht, F. Janata, and D. Schmidt. Determination of the Longitudinal and the Transverse Part in π^+ Electroproduction. *Nucl. Phys. B*, 137:294–300, 1978. doi:10.1016/0550-3213(78)90523-0.
- [19] P. C. Barry, L. Gamberg, W. Melnitchouk, E. Moffat, D. Pitonyak, A. Prokudin, and N. Sato. Tomography of pions and protons via transverse momentum dependent distributions, 2 2023.
- [20] Alexey Vladimirov. Pion-induced Drell-Yan processes within TMD factorization. *JHEP*, 10:090, 2019. doi:10.1007/JHEP10(2019)090.
- [21] Matteo Cerutti, Lorenzo Rossi, Simone Venturini, Alessandro Bacchetta, Valerio Bertone, Chiara Bissolotti, and Marco Radici. Extraction of pion transverse momentum distributions from Drell-Yan data. *Phys. Rev. D*, 107(1):014014, 2023. doi:10.1103/PhysRevD.107.014014.
- [22] José Manuel Morgado Chavez, Valerio Bertone, Feliciano De Soto Borrero, Maxime Defurne, Cédric Mezrag, Hervé Moutarde, José Rodríguez-Quintero, and Jorge Segovia. Pion generalized parton distributions: A path toward phenomenology. *Phys. Rev. D*, 105(9):094012, 2022. doi:10.1103/PhysRevD.105.094012.